Three-Dimensional Optical Data Storage Using Photochromic Materials

Satoshi Kawata[†] and Yoshimasa Kawata*[,‡]

Department of Applied Physics, Osaka University, Suita, Osaka, 565-0871, Japan, and Department of Mechanical Engineering, Shizuoka University, Johoku, Hamamatsu, 432-8561, Japan

Received June 14, 1999

Contents

1. Introduction

Optical memory storage devices such as compact disks (CD) and magnetooptical (MO) disks are becoming essential as audio and visual storage media as well as external computer data storage media. In these devices, a laser beam is used to record and read information. Since the laser spot can be focused to within 1 μm, higher densities and capacities can be achieved with optical memory than with conventional magnetic memory.

The data density achievable by optical memory devices is ultimately limited by the diffraction of electromagnetic waves. Present data-recording techniques have nearly attained this upper limit with commercially available CD and MO disks. Even utilizing an infinitely large objective lens with a high numerical-aperture (NA) value cannot reduce the bit data resolution distance for recording and reading to less than one-half the beam wavelength.

Consequently, current efforts to increase the memory density of optical devices are geared toward the development of durable short-wavelength compact lasers that emit blue or green light.[1−3] Doubling the frequency (or halving the wavelength) of the laser reduces the beam spot radius by 2, thereby increasing the density by 4 (when recorded in two dimensions). However, to increase the memory density to 100 times the current benchmark, laser diodes with output wavelengths 10 times shorter than those currently available would have to be employed. This requirement is obviously impossible because neither the laser materials nor the optical components, particularly the lenses, necessary to achieve this ultrashort wavelength can be manufactured in the 70−80 nm wavelength range. Another approach to increasing memory density is to use near-field optics.[4−8] This approach is reviewed in a separate review in this issue ("Diarylethene for Memories and Switches" by M. Irie).

A third approach, and one which promises to dramatically increase memory densities, is the development of photochromic materials.[9−13] These materials can undergo photon-mode recording, which is based on a photochemical reaction within the medium, as opposed to the heat-mode recording employed with the optical media currently in use. In photon-mode recording, light characteristics such as wavelength, polarization, and phase can be multiplexed to enable data storage and thus have the potential to dramatically increase the achievable memory density.

In this review we describe a method which utilizes photochromic materials[14−16] to overcome the current memory density limit by introducing an additional axial dimension to the recording process.[17−24] In this method, the z or longitudinal axis is utilized in addition to the surface dimension ($x-y$ space) of conventional optical memory. The data are thus written not on the material surface, but within the three-dimensional (3D) volume of the material.

This review focuses on recent developments in bit-oriented multilayered optical memories based on photochromic materials. Holographic memories are not included. The photochromic materials dealt with here are all synthetic ones. Biological photochromic materials are reviewed in a separate review ("Bacteriorhodopsin as a Photochromic Retinal Protein for Optical Memories" by N. Hampp).

2. Materials for 3D Memory

A photochromic compound is characterized by its ability to alternate between two different chemical forms having different absorption spectra, in response to irradiation by light of appropriate wave-

[†] Osaka University.
[‡] Shizuoka University.

10.1021/cr980073p CCC: $35.00 © 2000 American Chemical Society
Published on Web 04/25/2000

Satoshi Kawata was born in Osaka, Japan, in 1951. He received his B.S., M.S., and Ph.D. degrees all in Applied Physics from Osaka University in 1974, 1976, and 1979, respectively. From 1979 to 1981, he was with the University of California, Irvine, as a research associate. Since 1981, he has been with Osaka University, where he is currently a Professor of Applied Physics. He has been working in the fields of optics and spectroscopy, in particular micro- and nanoscale photonics. He has published several books and 150 original journals in near-field optics, surface plasmon polariton, two-photon microscopy, and other advanced laser microscopy, their applications to high-density optical data storage, photofabrication of microstructures, biomedical optics, and image and signal processing. He has organized several international conferences. He currently serves as the Editor of *Optics Communications* and as an Editorial Board member of several international journals. In Japan, He has served the Optical Society of Japan as the Vice President and the General Chair of the Annual Meeting in 1999. He was awarded the Japan IBM Science Award in 1996, the Louis Vuitton Moet Hennessy, Da Vinci Excellence Award in 1997, and the Ichimura Award in 1998, in addition to some others.

Yoshimasa Kawata was born in Fukushima, Japan, in 1963. He received his B.S., M.S., and Ph.D. degrees all in Applied Physics from Osaka University in 1987, 1989, and 1992, respectively. Subsequently, he held an Assistant Professor position in the Department of Applied Physics, Osaka University. Since 1997 he has been an Associate Professor at Shizuoka University. He is a member of the Editorial Board of the *Japanese Journal of Applied Physics*. His research interests are three-dimensional microscopy associated with nonlinear optics such as two-photon process, the photorefractive effect, and photoisomerization in organic molecules.

lengths. Photochromic materials are promising as recording media for optical memory because they erasably, or rewritably, store data in photon mode. Since the data-recording mechanism is based on the photochemical reaction of each molecule in the matrix, extremely high spatial resolution should be achievable.

The following properties are required of photochromic materials which are to be employed as optical

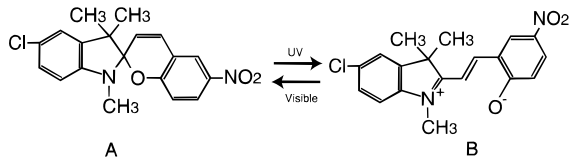

Figure 1. Chemical structure of spirobenzopyran. A and B are spirobenzopyran isomers.

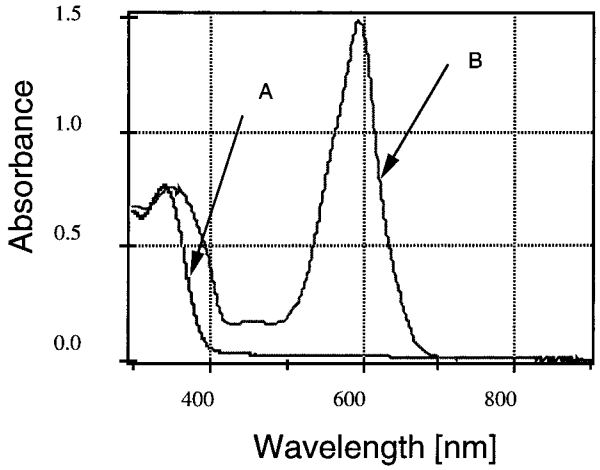

Figure 2. Absorption spectra of a polystyrene film containing spirobenzopyran both before (A) and after (B) exposure to 442-nm light.

memory media: (1) thermal stability of both isomers, (2) resistance to fatigue during cyclic write and erase processes, (3) fast response, (4) high sensitivity, and (5) nondestructive readout capability.

For 3D recording, a large two-photon absorption coefficient is preferred because 3D memory essentially uses a two-photon process to access a point within the volumetric medium. In the following section, typical photochromic compounds used for 3D memories will be described.

2.1. Spirobenzopyran Derivatives

Rentzepis et al.[17] first demonstrated a bit-oriented 3D optical memory system using a photochromic spirobenzopyran, shown in Figure 1. Isomer A has an absorption band shorter than 450 nm and, upon irradiation with ultraviolet (UV) light, it converts to isomer B, which has an absorption band around 600 nm, as shown in Figure 2. Isomer B fluoresces around 700 nm upon photoexcitation with 500−700 nm light.

Figure 3 illustrates the principle of 3D optical memory based on a two-photon process proposed by Rentzepis et al.[17,25,26] They used two beams to access a point in a volumetric recording medium. For writing data, which required excitation in the ultraviolet range, a two-photon absorption involving either a 1064 and a 532 nm photon (corresponding to 355 nm excitation) or two 532 nm photons (corresponding to 266 nm excitation). At the intersection of the two beams, isomer A absorbed two photons simultaneously and photoisomerized to isomer B.

A similar two-photon process was employed for reading data. When isomer B molecules were excited by the absorption of two 1064 nm photons, the excitation caused only the written molecules to fluoresce. Although this fluorescence readout method

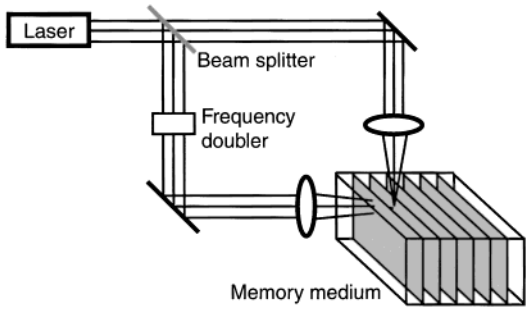

Figure 3. Principle of 3D optical memories as proposed by Rentzepis et al.[17]

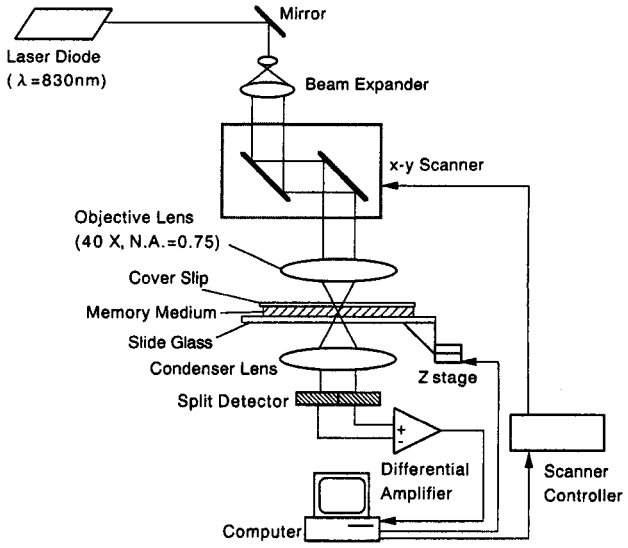

Figure 4. Optical system for the readout of 3D memory. A near-IR differential phase-contrast microscope was used for nondestructive readout.

is sensitive, the memory was erased during the reading process, due to partial occurrence of the reverse reaction from photoexcited isomer B to isomer A. Unfortunately, a destructive readout method such as this is not practical. The development of nondestructive readout methods is essential if this system is to become practical.[12−16] Thus, the most promising method is to read the memories by detecting the refractive-index changes that accompany the photoisomerization induced by long-wavelength light. This readout method does not induce photochromic reactions.

Nondestructive readout was demonstrated using a small difference in the refractive index of the spirobenzopyran isomers (Figure 1) in the near-IR.[14] The small refractive-index change was detected using a near-IR laser-scan differential phase-contrast microscope (Figure 4). The two isomers of the spirobenzopyran have very different absorption spectra, which suggests that the isomers also have different refractive indices. In the near-IR region around 800 nm, both isomers have negligible absorption. Therefore, the near-IR light needed to read the change of refractive index does not stimulate the photochromic photoreaction.

Data were recorded by focusing laser light (441.6 nm) on the two layers, which were separated by as much as 70 μm, using a laser scanning microscope

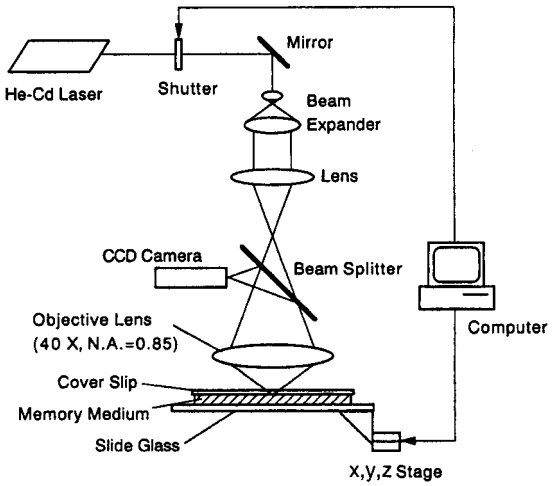

Figure 5. Optical setup for recording 3D bit information in photochromic memory.

as shown in Figure 5. Bit sequences of 24 × 24 bits per layer which formed the letters "A" and "B" were obtained. The bit interval was 5 μm × 5 μm in each layer, and the separation distance between layers was 70 μm.

Figure 6 shows the readout from the two layers. The crosstalk between the layers was small enough to allow the recorded data to be clearly read by the differential phase-contrast microscope. Since the signal intensity was proportional to the derivative of the refractive index, the readings at the edges of the bits were slightly enhanced. The scanning rate was 1 layer per s, and the readout could be repeated more than 7000 times without destroying the recorded information. The difference in the refractive indices of the two isomers was measured to be 0.02 at 830 nm.[27] Unfortunately, the spirobenzopyrans used in the above system have poor durability and the photogenerated isomers were thermally unstable.

Spirobenzopyran derivatives also were utilized as the media for wavelength-multiplexed memory systems.[11,28,29] A narrow absorption band is required for the wavelength multiplex to work. This narrow spectrum was obtained by using J-aggregates of spirobenzopyrans.[29] The J-aggregates have absorption peak widths of a few tens of nanometers. A five-wavelength multiplexed memory was demonstrated using these J-aggregates, but considerable crosstalk between the multiplexed channels was observed.[11]

2.2. Diarylethene Derivatives

Figure 7 shows two diarylethene derivatives containing heterocyclic rings, specifically (a) 1,2-bis(2-methyl-1-benzothiophen-3-yl) perfluorocyclopentene and (b) 2-(1,2-dimethyl-3-indolyl)-3-(2,4,5-trimethyl-3-thienyl)maleic anhydride.[13,30] These compounds do not exhibit thermochromicity even at 200 °C, and their colored, closed-ring forms are stable for more than 3 months at 80 °C. Furthermore, the cyclization/ring-opening reaction cycle can be repeated more than 10^4 times without the loss of photochromic performance. Thus, diarylethene derivatives of this type currently are the most promising photochromic

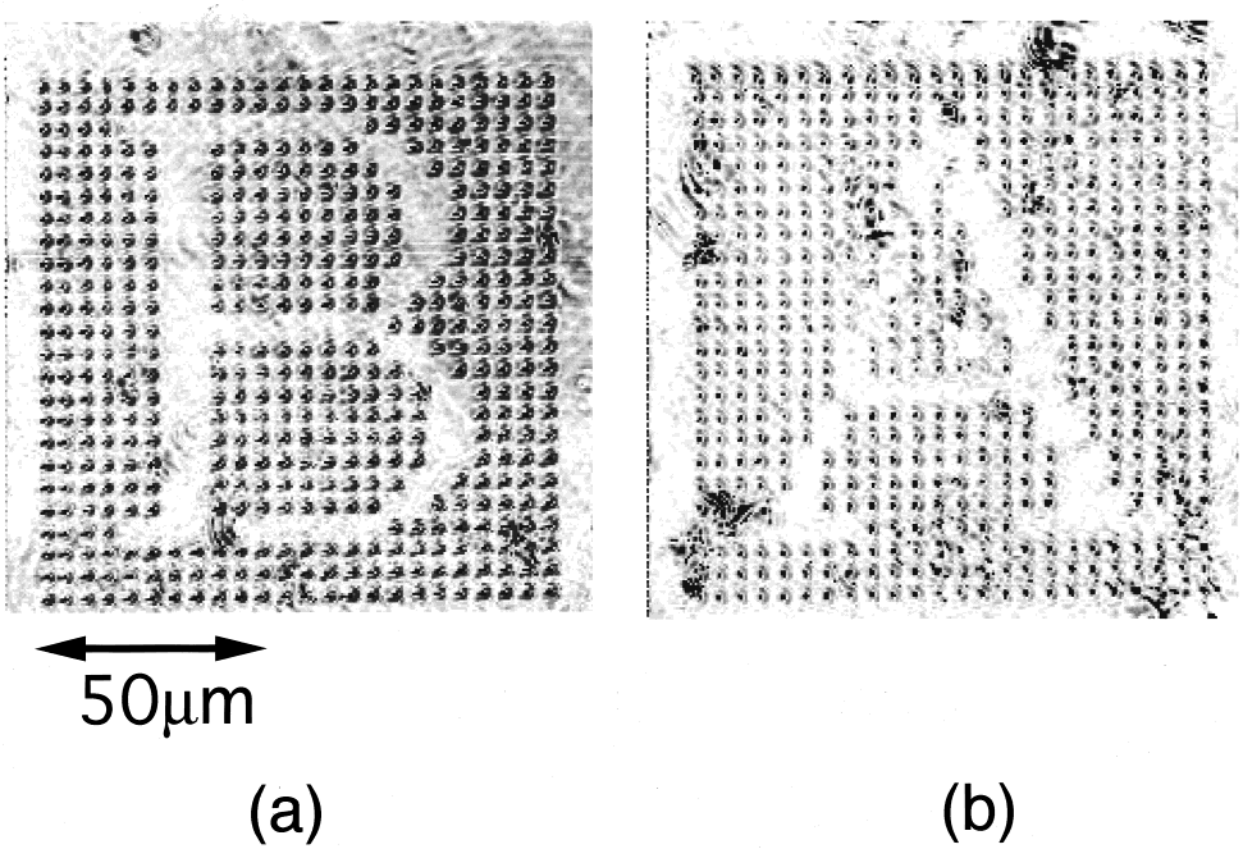

Figure 6. Bit patterns read from photochromic memory using near-IR laser-scanning differential phase-contrast microscopy: (a) first layer, (b) second layer. The bit interval is 5 μm, and the layer distance is 70 μm.[14]

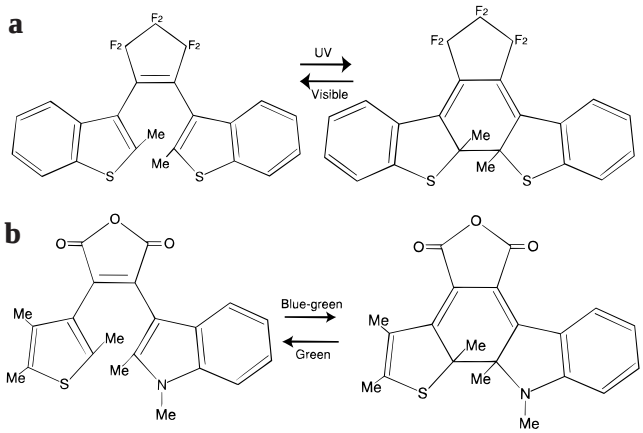

Figure 7. Photochromic reactions of (a) 1,2-bis(2-methyl-1-benzothiophen-3-yl)perfluorocyclopentene and (b) 2-(1,2-dimethyl-3-indolyl)-3-(2,4,5-trimethyl-3-thienyl)maleic anhydride.

compounds for use as high-density optical memory media.

Poly(methyl methacrylate) containing *cis*-1,2-dicyano-1,2-bis(2,4,5-trimethyl-3-thienyl)ethene (B1536) was used as a photochromic optical memory medium.[15,16] Figure 8 shows the chemical structures of the two isomers of B1536, along with their absorption.[15]

Unexcited B1536 exists as a yellow isomer that is converted into a red isomer upon irradiation with 380 nm light. The data written in this manner can be erased by irradiating the medium with 543 nm light.

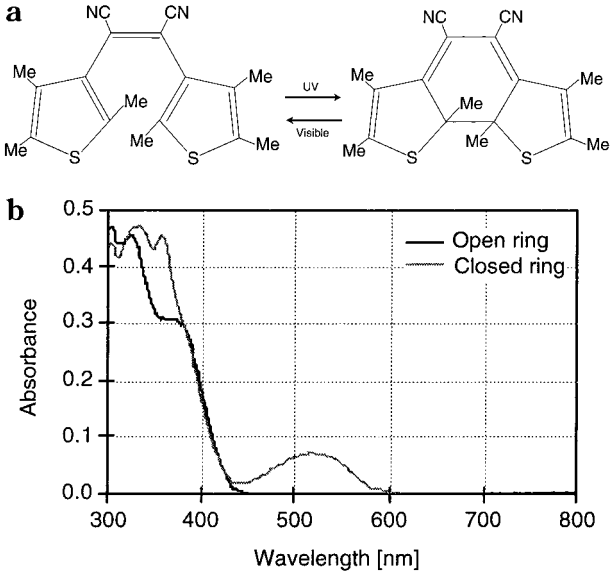

Figure 8. (a) Chemical structures of *cis*-1,2-dicyano-1,2-bis(2,4,5-trimethyl-3-thienyl)ethene (B1536) and (b) its absorption spectra.

This photochromic material (B1536) did not exhibit any apparent fatigue, even after 100 write/erase cycles. Furthermore, the written data (e.g., the red isomers) were stable at 80 °C for more than 3 months, and the thermal back-reaction (from the red isomer to the yellow isomer) did not occur, even at 200 °C.[31]

A two-photon process which focused on a point in the thick medium was used to record the data. A 760

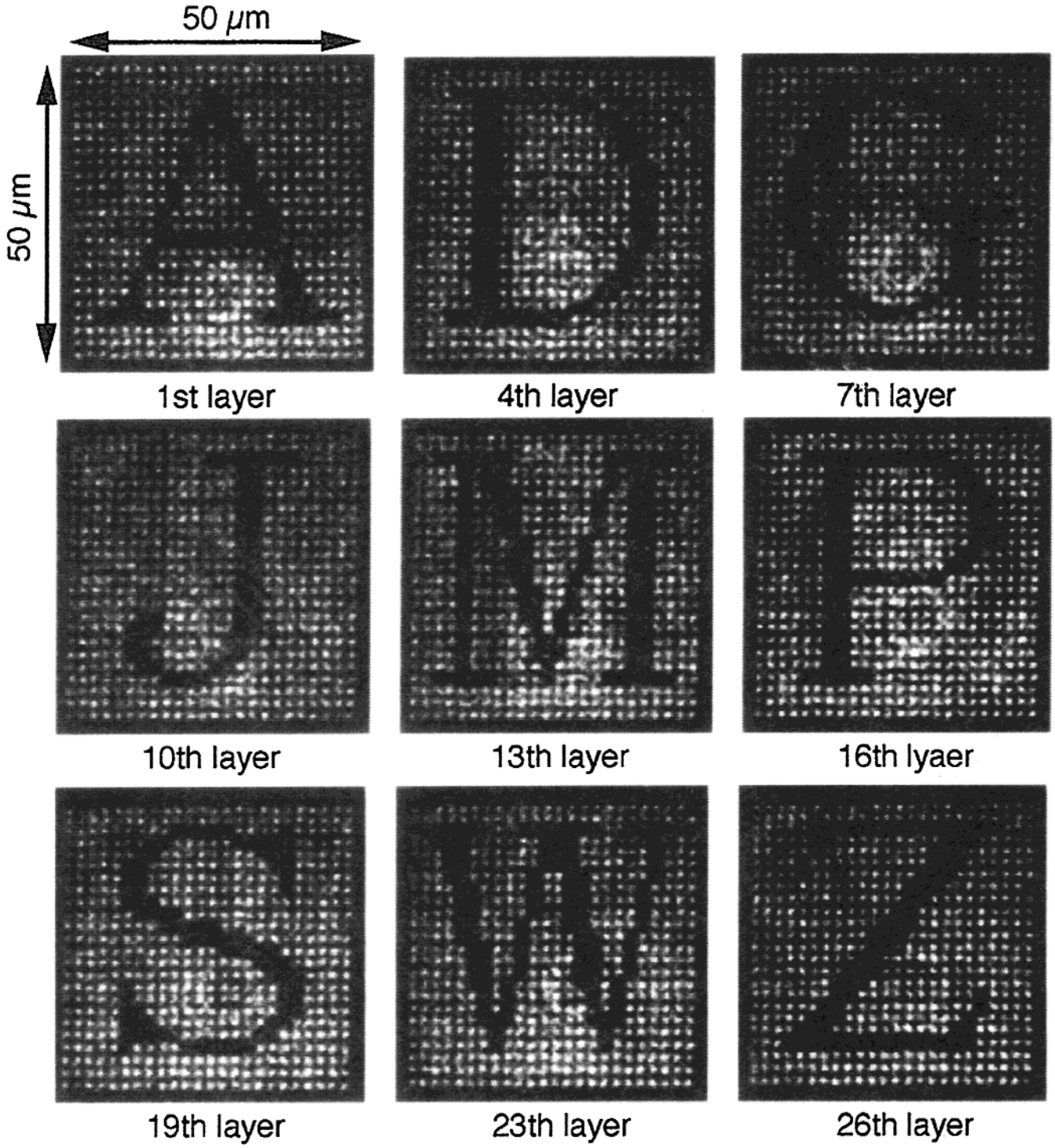

Figure 9. Readouts of bit patterns written into photochromic memory using a diarylethene derivative. The data were read using a reflection confocal microscope.[16]

nm Ti:sapphire laser operated in mode-locked pulsed laser mode was employed as the recording light source. Since the probability of two-photon absorption occurring is proportional to the squared intensity of the incident light, photoisomerization is only induced at the focal point, where the intensity is very high.[17,18,22,32,33] This technique is attractive for recording data in an erasable medium because it allows information to be written onto a particular layer without erasing the data already written on neighboring layers.

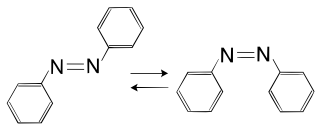

Figure 10. Photoinduced isomerization of azobenzene.

Figure 9 shows readout images of the bits written in 26 consecutive layers. The bit and layer intervals were 2 and 5 μm, respectively. The data were read using a reflection confocal microscope (RCM). The details of this readout system are discussed in the

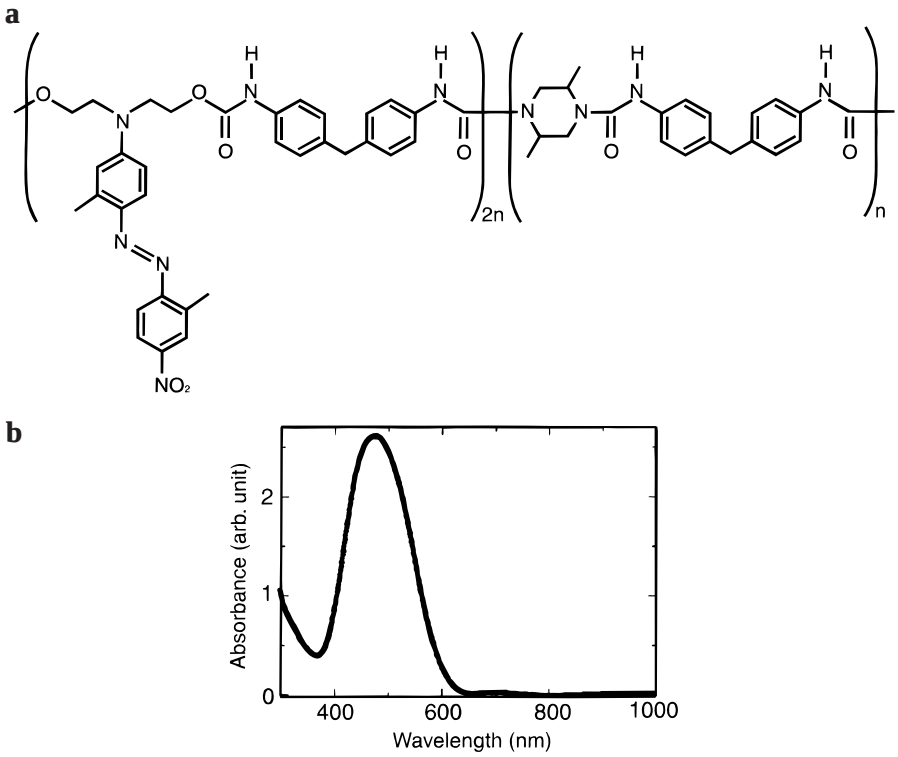

Figure 11. (a) Chemical structure of the urethane−urea copolymer and (b) its absorption spectrum.

Optics section. With the RCM, the written data are clearly readable without crosstalk.

2.3. Azobenzene Derivatives

Azobenzene derivatives constitute a family of dye molecules which are well-known for their photochromic properties. These properties are due to reversible cis−trans photoisomerizations which the derivatives undergo.[34−37] Figure 10 shows the photoisomerization process exhibited by azobenzene. Azobenzene derivatives have two geometric isomers: a trans form and a cis form. The isomerization reaction that interconverts these two isomers may be light- or heat-induced. The trans form is generally more stable than the cis form, thus the thermal isomerization usually occurs from the cis to the trans form. However, light induces transformations in both directions.

A new material, a urethane−urea copolymer with azo-dye side chains, was recently demonstrated to be useful as a 3D optical memory material.[38] Figure 11a shows the chemical structure of the urethane−urea copolymer. This urethane−urea copolymer was originally developed to be a nonlinear optical waveguide.[39,40] The copolymer has a relatively high optical nonlinearity and is stable at room temperature. Its azo-dye side-chain structure allows it to semifix chromophores for use as photosensitizers in the optical memory read/write process.

The absorption spectrum of the copolymer shows a maximum at 476.3 nm and a small absorption in the region above 600 nm (Figure 11b). Upon illumination with blue light, the azo dye undergoes a cis−trans isomerization which produces a refractive-index change on the order of 10^{-2}.

Another recording medium was developed by alternately coating photosensitive films (urethane−urea copolymer) and nonphotosensitive films (poly(vinyl alcohol), PVA) on a glass substrate. Figure 12 shows the structure of the multilayered recording medium.

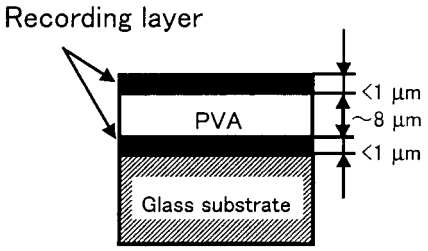

Figure 12. Multilayered recording medium in which photosensitive films and nonphotosensitive transparent PVA films are alternately stacked.

The axial distribution of the data recorded on this medium is shown in Figure 13. This figure was reconstructed from a set of images captured as the focus plane was changed. The three cross-sections, which were taken along the optical axis and along the first and second layers, respectively, are also shown in Figure 13. The two recording layers were clearly detected, and the bit data were also clearly recognized. The side lobes which appear in the cross-section taken along the optical axis were due to aberrations in the objective.

This two-layered optical memory system produced a readout result which is shown in Figure 14. The readout was accomplished using a reflection-type confocal microscope. A He−Ne laser was used as the light source during reading, because the urethane−urea copolymer does not absorb red light well. The recorded bit data produced scattered light due to its refractive-index change, and this was detected using a photomultiplier tube (PMT). A "1" pattern was formed by the bit sequences in the first layer, while

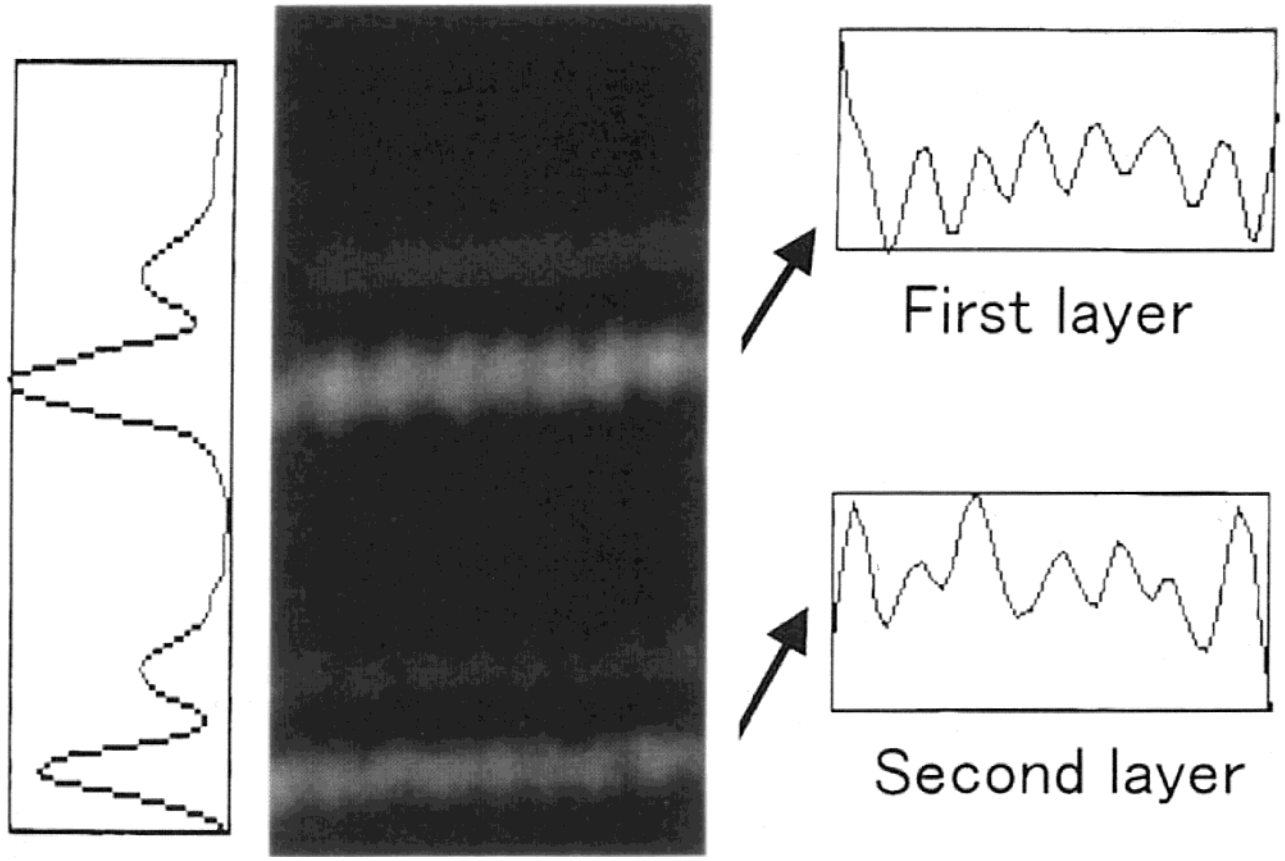

Figure 13. Axial distribution of the data recorded in the two-layer medium. The data were read using a reflection confocal microscope.[38]

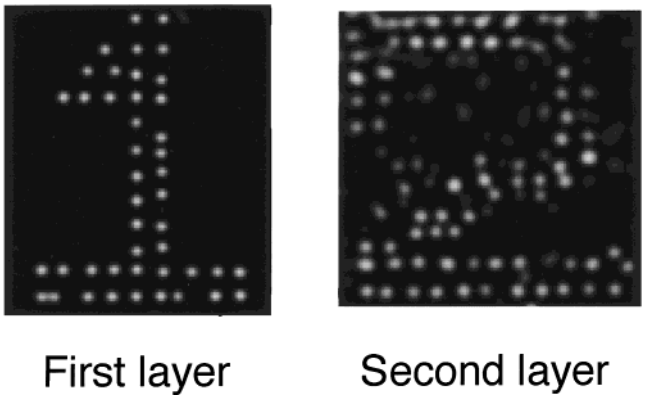

Figure 14. Data recording and reading results from the two-layer medium. The distance between neighboring bits is 3 μm, and the distance between layers is about 8 μm.

a "2" pattern was formed in the second layer. The degradation observed in the second layer was due to inhomogeneity within that layer. The distance between bits in the layers was 3 μm, and the distance between layers was about 8 μm.

3. Optics

3.1. Single-Photon Recording

Although two-photon excitation is the most desirable method for bit-data recording in 3D optical memories, single-photon recording also is an acceptable method since it gives good separation between the recorded planes. Figures 6 and 14 show data recorded using a single-photon process. A typical system for single-photon recording is shown in Figure 5. A He−Cd laser of 441.6 nm wavelength was used to record on the spirobezopyran medium (Figure 1), and an Ar^+ laser of 488.0 nm was used to record on the urethane−urea copolymer medium (Figure 11a). Crosstalk between the layers was negligible in both cases.

Since single-photon recording does not require ultrashort-pulse lasers, conventional semiconductor lasers can be used. Thus, the optical systems utilized for recording in CD and MO devices can be readily applied to 3D optical memory recording.

3.2. Single-Beam, Two-Photon Recording

One reason two-photon excitation is preferable for recording in 3D optical memory systems is because crosstalk between two adjacent layers is much reduced with this method. Another advantage of two-photon excitation is that it reduces multiple scattering. This reduction occurs because the illumination beam that is utilized has an infrared wavelength.

A typical optical recording system for single-beam, two-photon recording is similar to the one-photon recording system shown in Figure 5, except that it uses a different light source. In the system shown in Figure 5, a Ti:sapphire laser was used as the light source because this laser can provide the high peak-power light which the cooperative nature of the two-photon excitation requires to produce efficient excitation.[18,32] Other systems have been developed using a mode-locked Ti:sapphire laser,[16,33,41,42] a mode-

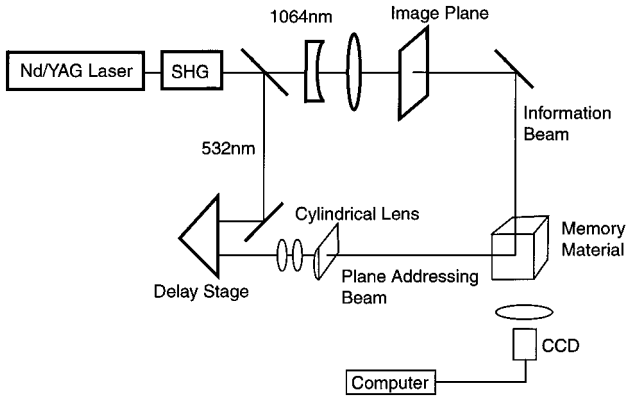

Figure 15. Experimental setup for recording and reading information using two beams.[43] The resulting two-dimensional image is stored in the plane where the plane-addressing beam and information beam intersect.

locked dye laser,[18] and a mode-locked YAG laser.[17,43] Continuous-wave light also has been investigated as a means of producing the two-photon process.[44,45] A high numerical-aperture lens is required to achieve separation of the layers, since this allows focusing on a well-confirmed spot at a point in a thick medium.

The disadvantage of ultrashort-pulse lasers is that they increase the cost of the recording device and make it difficult to produce a compact system. Recently, a compact ultrashort-pulse laser in which an Er-doped fiber was used as the resonator was developed.[46−49] Semiconductor lasers operated in mode-lock are also under investigation.[50−52] Thus, the cost and the size of ultrashort-pulse lasers will decrease soon.

3.3. Right-Angle, Two-Beam, Two-Photon Recording

Rentzepis et al. have demonstrated a 3D memory device which uses two right-angle beams to access a point in a volumetric medium as shown in Figure 3.[17,21,43] While this system clearly demonstrated that bit-oriented 3D memory storage can be achieved in this manner, its disadvantages are that the two beams are difficult to align such that they intersect at the same point and that the working distance of the objective lenses are limited. Higher density storage was achieved using high NA objective lenses; however, the small working distances of the lenses still made it difficult to achieve the necessary right-angle configuration.

To solve these problems, Rentzepis et al. proposed to use one beam as a plane addressing beam. Figures 15 and 16 show the experimental system for writing and reading data in 3D using this technique and its result, respectively. The SHG light of a YAG laser was used for the addressing beam, while 1.06 μm wavelength light was used to carry the data. In this manner, they succeeded in recording 100 layers with intervals of 30 μm per layer and of 80 μm between layers.

3.4. Confocal Phase-Contrast Microscope

As described in section 2.1, the detection of refractive-index changes between two isomers in a photochromic material is the most promising technique for nondestructive data readout in these systems.[14] This requires that a readout system that is sensitive to refractive-index distribution should be developed. Several applicable systems, including as a phase-contrast microscope, a differential phase-contrast microscope, and a reflection confocal microscope have been proposed.

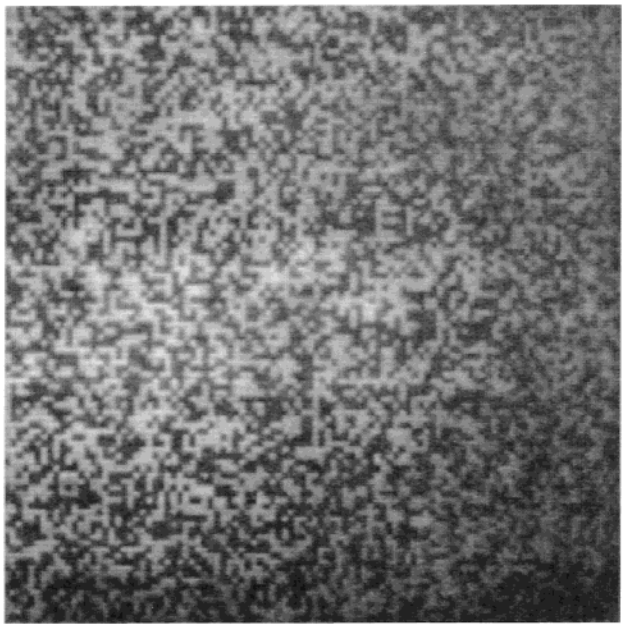

Figure 16. One of the 100 data images stored as the result of right-angle, two-beam, two-photon recording. The interval between neighboring bits is 30 μm per layer and between layers is 80 μm.[21]

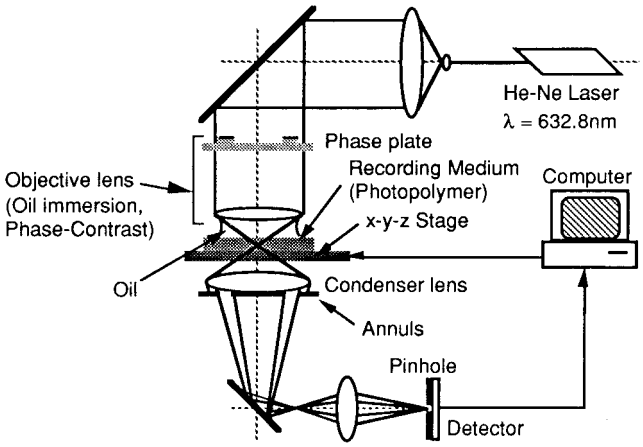

Figure 17. Confocal phase-contrast microscope for 3D memory.

Figure 17 shows a laser-scanning confocal microscope for phase-contrast imaging. Illumination by a point light source reduces the occurrence of unnecessary scattered light. The confocal microscope's point detector detects the light intensity from only a specific point of interest in the thick sample. Thus, it reads only the light intensity associated with the conjugate pair at the point of interest in the thick volume (or the focused point of the laser beam in the volume). The scattered light produced by other non-focused points does not contribute to the detected signal. Hence, the signal contrast obtained for the

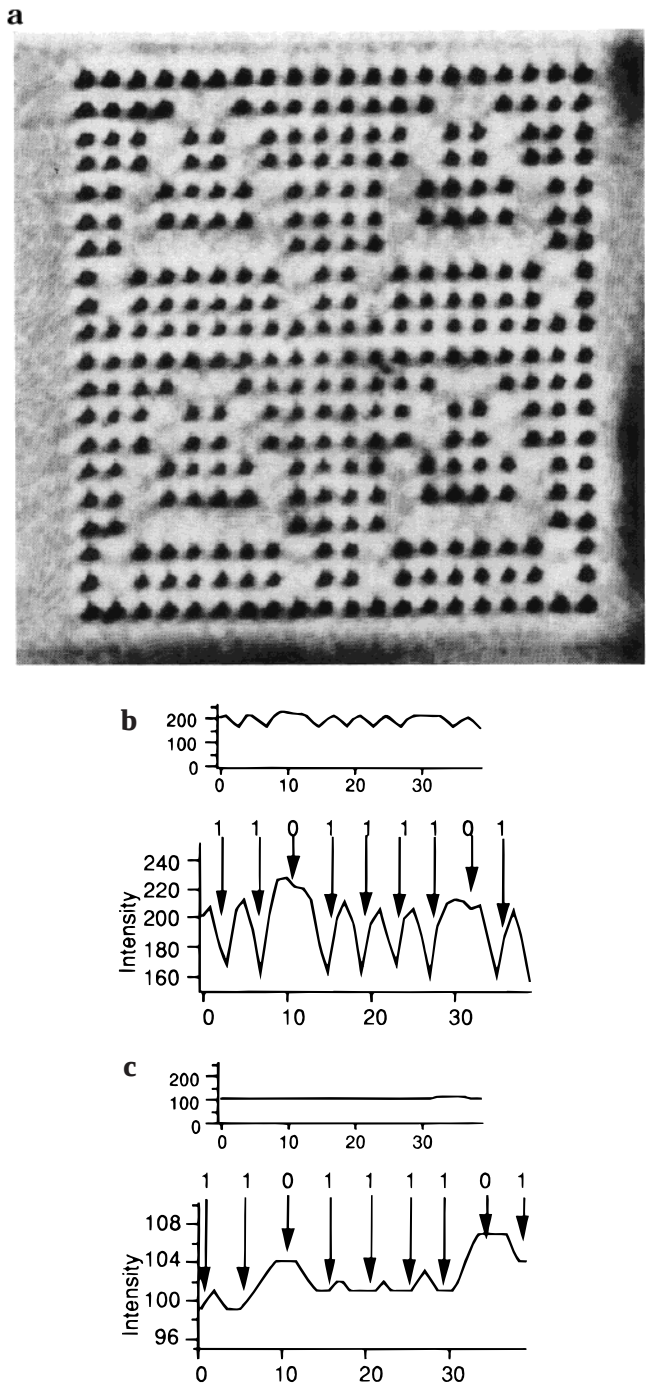

Figure 18. (a) Readout data obtained using a confocal phase-contrast microscope and (b) its cross section. (c) Cross section of the same area read using a conventional phase-contrast microscope.

images is excellent and the crosstalk between planes is negligible compared with those obtained using a nonconfocal microscope. Better spatial resolution also is obtained when using the confocal microscope because of its nonlinear spatial response (which is the product of illumination point-spread functions and the detection amplitude point-spread function).[53−55]

Figure 18a presents an example of bit data read using a confocal microscope. A He−Ne laser (632.8 nm) was used in this system, together with a phase-contrast objective and an annular pupil for phase-contrast (dark field) imaging. Figure 18b shows a partial cross-section of the readout data. For comparison, the same segment of the data was read using a conventional microscope with the same objective lens (Figure 18c). The results clearly demonstrate the advantages of confocal microscopy for high-contrast and high-resolution imaging within these 3D structures.

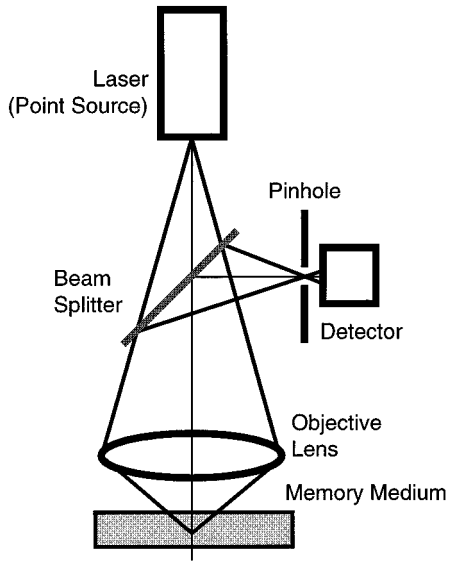

Figure 19. Typical optical setup for a reflection confocal microscope.

3.5. Differential Phase-Contrast Microscope with a Split Detector

A scanning differential phase-contrast microscope with a split detector, as shown in Figure 4, provides an alternative readout system. The optical configuration of this system is compact and easy to align. The memory medium containing recorded data bits is located at the focus of an objective lens. The band limit of the optical transfer function (OTF) was found to be the same as that of a conventional microscope with incoherent illumination,[56] while the resolution, especially the axial resolution of the phase-contrast microscope, was similar to that obtained by Zernike's phase-contrast microscope. However, the contrast of the image was much improved over that obtained with Zernike's phase-contrast microscope, because the nondiffracted components were completely eliminated through subtraction of the signals between the two detectors. This readout system was therefore sensitive to small phase changes.

3.6. Reflection Confocal Reading

The reflection confocal microscope (RCM) provides another type of readout system for multilayered optical memories. This system is attractive because it has an extremely high axial resolution and its configuration is much simpler than these of the transmission confocal microscopes. A typical RCM system is shown in Figure 19.

One disadvantage of the transmission confocal microscopes that are equipped with phase-reading systems is that their focus deviates from the pinhole

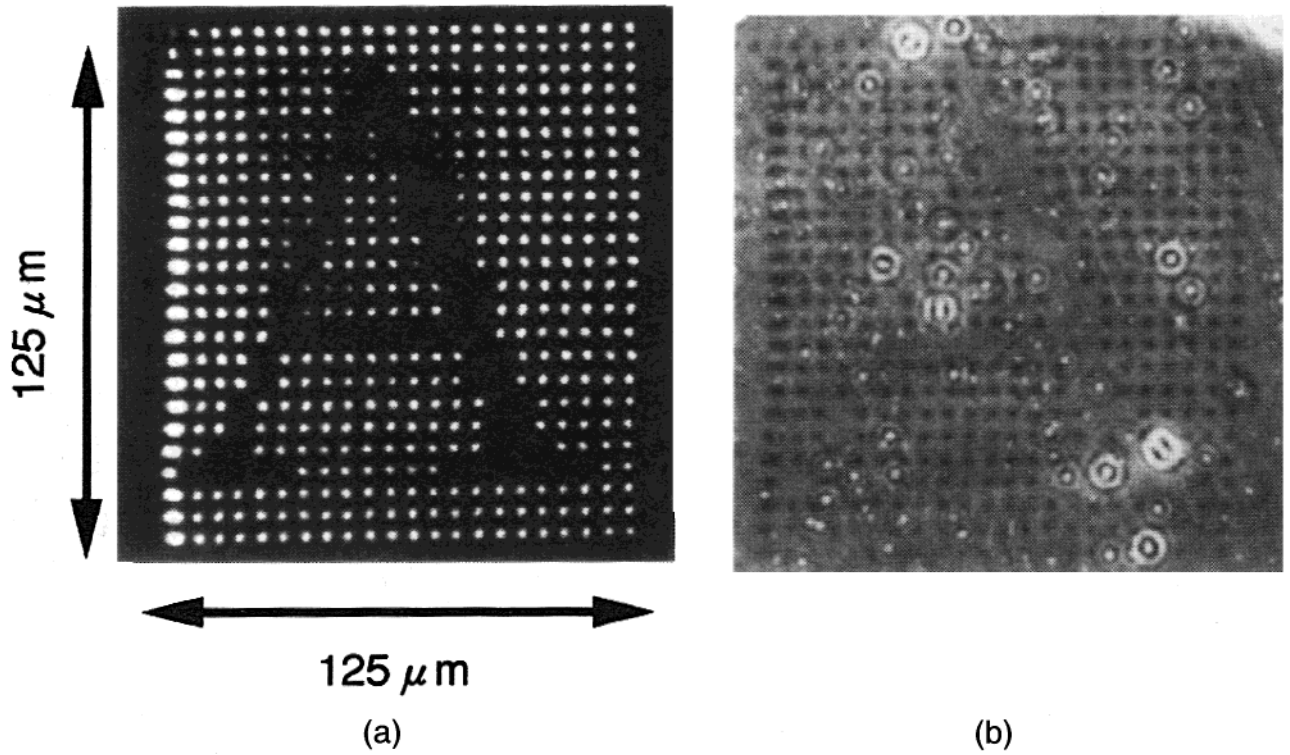

Figure 20. Comparison of data read using (a) a RCM and (b) a transmission microscope.

due to the inhomogeneity of the refractive index, the thickness of the memory medium and substrate, or both. As a result, the detected signal has a background which arises from local inhomogeneities in the medium and the substrate.

The use of an RCM system alleviates this problem because the beam that is reflected at the data bit arrives at the pinhole even in the presence of inhomogeneity. RCMs, however, have not been used for reading 3D-stored data, mainly because their reading optics' 3D spatial-frequency band does not necessarily match the writing optics' 3D band.

When the appropriate optical parameters are chosen, including the NAs of the objective lenses and the wavelengths of the writing and reading lights, a common spatial band results for both writing and reading in three dimensions. Figure 20a,b shows data readouts obtained with an RCM and a transmission phase-contrast microscope, respectively. The bit-data image obtained with the reflection readout system clearly is much better than that obtained with the transmission readout system.

Figure 21 shows the spatial-frequency band of a written bit in relation to the transfer function band of the reading system.[57−60] This figure shows a vertical slice of the 3D band residing in the 3D band of the transfer function (*k*-vector) space that includes the axial frequency ($1/z$). $1/r$ is the transaxial spatial frequency of the polar coordinate $r = \sqrt{(x^2 + y^2)}$, where x and y are the two-dimensional coordinates of the transaxial plane. The shaded regions represent the spatial-frequency components of the two-photon writing optics and the 3D Fourier transform of a bit profile formed using the two-photon process with focused optics. The ellipse in Figure 21 is a vertical slice of a bun-shaped band that exists in three

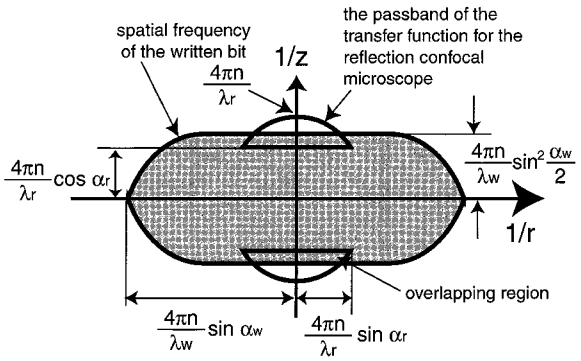

Figure 21. Writing optics band for a two-photon process, and the reading optics band for RCM.

dimensions. This band is obtained by 3D autocorrelation of a doughnut-shaped band that represents a 3D spatial-frequency band arising from the single-photon-focused optics. The NAs of the objective lenses used in writing and reading are given by $n \sin \alpha_w$ and $n \sin \alpha_r$, respectively, where n is the refractive index of the recording material and α_w and α_r are the maximum semiangles of the objectives. λ_w and λ_r are the wavelengths used for writing and reading, respectively. The 3D spatial-frequency band expands when λ_w decreases or $n \sin \alpha_w$ increases. The parabolas (one of which is concave up and one of which is concave down) shown in Figure 21 are vertical slices of the reading optics band of the RCM. These parabolas are semicylindrical in 3D space. The reading optics band is also given by the NA of the objective lens and the wavelength λ_r. The written data can be read when there is a common area (actually a common volume) in the 3D frequency bands for both writing and reading. Appropriate values of $n \sin \alpha_w$, $n \sin \alpha_r$, λ_w, and λ_r can be selected

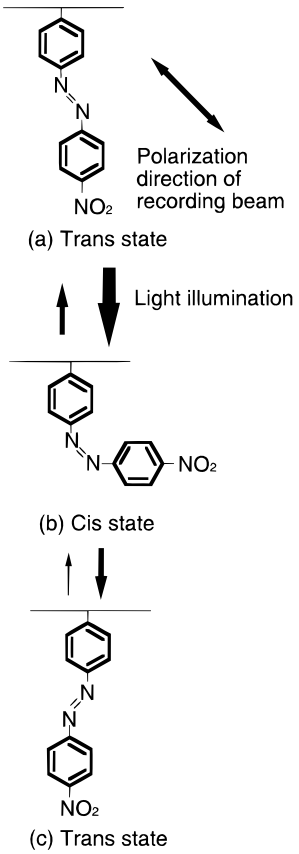

Figure 22. Mechanism for the generation of anisotropy during the photoisomerization of the urethane−urea copolymer.

to make the bun and the crescents overlap. Objective lenses with very high NAs must be chosen in order to create an overlap between the bands of both the writing and reading optical systems. For example, when NA = 1.4 is used for writing, a NA higher than 1.2 is required for reading (λ_w = 760 nm and λ_r = 633 nm).

3.7. Polarization Reading

It is well-known that upon irradiation with linearly polarized blue or green light, the azo-dye chromophores can undergo trans−cis photoisomerization to induce an anisotropic or uniaxial orientation of polymer side groups.[61] Figure 22 shows a schematic diagram of the polarized light-induced photoisomerization of an azo dye attached to a urethane−urea copolymer (Figure 11a). The trans state of the azo dye, which is shown in Figure 22a, absorbs light that is polarized parallel to its dipole moment. This causes it to flip-flop to the cis isomer, which is shown in Figure 22b. The cis isomer also absorbs blue and green light and photoisomerizes back to the trans isomer. There are two possible outcomes from the cis− trans photoisomerization: one is the regeneration of the state which existed prior to the illumination, and the other is the generation of an inverted trans state where the axis of the isomer is rotated 90° from its initial state, as shown in Figure 22c.[62,63] This trans isomer absorbs less light than the trans isomer shown in Figure 22a because the direction of the trans isomer shown in Figure 22c is nearly perpendicular to the polarization of the illuminating light. The trans and cis chromophores interconvert in a manner which results in the number of trans states (a) decreasing and the number of trans states (c) increasing during their continued exposure to the linearly polarized light. It is this increase in the number of azo dyes whose axes are perpendicular to the direction of the illuminated polarization that generates the optical anisotropic refractive-index distribution.[64,65]

Figure 23a shows the readout results for bit data that were recorded on the azo-dye material using with a polarization angle of from 0° to 180° and a pitch of 15°. The two vertical dots were recorded using identical polarization states, while the data were read out using four polarization states. An Ar^+ laser (514.5 nm) was used during recording, and readout was carried out using white light. It was noted that the reading intensity was highest when the polarization angles of the recording and reading beams were perpendicular. This confirmed that the azo-dye molecules were oriented perpendicular to the polarization of the Ar^+ laser light.

Figure 23b shows the polarization-multiplexed recorded data "X", "Y", and "Z" at the respective recording polarization angles of 0°, 60°, and 120°. Each pattern was recorded using the same exposure time. The lateral distance between bits in the plane was 3 μm, and the expected refractive-index change was estimated to be about 0.01.

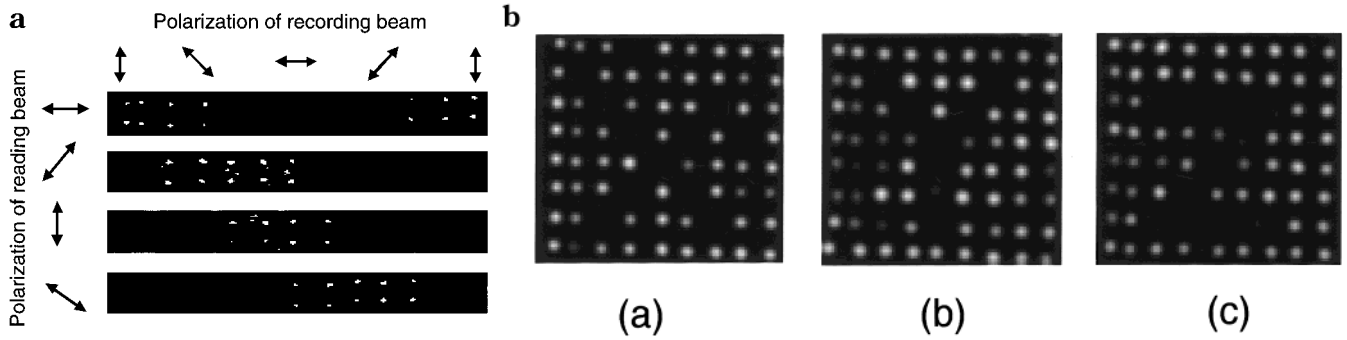

Figure 23. Writing and reading with various light polarization directions: (a) the readout results for data that were recorded with polarization angles from 0° to 180° and a pitch of 15°. The data were read using four polarization states. (b) The readout results from polarization-multiplex-recorded data at recording polarization angles of 0°, 60°, and 120°, respectively.

4. Concluding Remarks

Various optical systems for reading and writing 3D memories using photochromic materials were presented. The use of photochromic materials in 3D memory system is desirable because they present several major advantages over current optical systems, including their erasable/rewritable capability, high resolution, and high sensitivity. Several photochromic materials having adequate properties as 3D memory recording media were described. The 3D recording techniques which were described compliment, rather than conflict with, other techniques for achieving high-density memory storage, such as wavelength multiplexing, polarization multiplexing, and wavelength shortening. Combining these techniques results in increased storage density. Utilizing two-photon excitation is key to achieving effective 3D memory systems. Thus, photochromic materials with large two-photon absorption coefficients must be developed.[66] The multilayered memory which defines 3D memory systems is just an extension of conventional optical memories into the *z*-direction, so the scanning, tracking, and auto-focusing techniques used in conventional memory systems can be adapted to work with 3D systems as well.

5. Acknowledgments

The authors deeply appreciate Professor M. Irie of Kyushu University for his valuable comments on this review.

6. References

(1) Haase, M. A.; Qui, J.; DePuydt, J. M.; Cheng, H. *Appl. Phys. Lett.* **1991**, *59*, 1272.
(2) Nakamura, S.; Mukai, T.; Senoh, M. *Appl. Phys. Lett.* **1994**, *54*, 1687.
(3) Nakamura, S.; Senoh, M.; Iwasa, N.; Nagahamai, S. *Jpn. J. Appl. Phys.* **1995**, *34*, L797.
(4) Pohl, D. W.; Denk, W.; Lanz, M. *Appl. Phys. Lett.* **1984**, *44*, 651.
(5) Betzig, E.; Lewis, A.; Harrotunian, A.; Isaacson, M.; Kratschmer, E. *Biophys. J.* **1986**, *49*, 269.
(6) Betzig, E.; Trautman, J. K.; Wolfe, R.; Gyorgy, E. M.; Finn, L. *Appl. Phys. Lett.* **1992**, *61*, 142.
(7) Martin, Y.; Rishton, S.; Wickramashinghe, H. K. *Appl. Phys. Lett.* **1997**, *71*, 1.
(8) Tsujioka, T.; Irie, M. *Appl. Opt.* **1998**, *37*, 4419.
(9) Hiershberg, Y. *J. Am. Chem. Soc.* **1956**, *78*, 2304.
(10) Irie, M.; Uchida, K. *Bull. Chem. Soc. Jpn.* **1998**, *71*, 985.
(11) Hibino, J.; Moriyama, K.; Suzuki, M.; Kishimoto, K. *Thin Solid Films* **1992**, *210/211*, 562.
(12) Uchida, K.; Irie, M. *J. Am. Chem. Soc.* **1993**, *115*, 6442.
(13) *Photoreactive Materials for Ultrahigh-Density Optical Memory*; Irie, M., Ed.; Elsevier: Amsterdam, 1994.
(14) Toriumi, A.; Herrman, J. M.; Kawata, S. *Opt. Lett.* **1997**, *22*, 555.
(15) Toriumi, A.; Kawata, S.; Gu, M. *Proc. Jpn. Soc. Laser Microsc.* **1998**, *22*, 24.
(16) Toriumi, A.; Kawata, S.; Gu, M. *Opt. Lett.* **1998**, *23*, 1924.
(17) Parthenopoulos, D. A.; Rentzepis, P. M. *Science* **1989**, *24*, 843.
(18) Strickler, J. H.; Webb, W. W. *Opt. Lett.* **1991**, *16*, 1780.
(19) Piyaket, R.; Cokgor, I.; Esener, S. C.; Solomon, C.; Hunter, S.; Ford, J. E.; Dvornikov, A. S.; Tomov, I.; Rentzepis, P. M. *Proc. SPIE* **1994**, *2297*, 435.
(20) Cokgor, I.; McCormick, F. B.; Dvorkikov, A. S.; Wang, M. M.; Kim, N.; Coblentz, K.; Esener, S. C.; Rentzepis, P. M. *Proc. SPIE* **1997**, *3109*, 182.
(21) Wang, M. M.; Esener, S. C.; McCormik, F. B.; Cokgor, I.; Dvornikov, A. S.; Rentzepis, P. M. *Opt. Lett.* **1997**, *22*, 558.
(22) Kawata, S.; Toriumi, A. *Proc. SPIE* **1997**, *3109*, 174.
(23) Akimov, D. A.; Fedotov, A. B.; Koroteev, N. I.; Levich, E. V.; Magnitskii, S. A.; Naumov, A. N.; Sidorov-Biryukov, D. A.; Sokolyuk, N. T.; Zheltikov, A. M. *Opt. Mem. Neural Networks* **1997**, *6*, 31.
(24) Pudavar, H. E.; Joshi, M. P.; Prasad, P. N.; Reinhardt, B. A. *Appl. Phys. Lett.* **1999**, *74*, 1338.
(25) Parthenopoulos, D. A.; Rentzepis, P. M. *J. Appl. Phys.* **1990**, *68*, 5814.
(26) Dvornikov, A. S.; Rentzepis, P. M. *Opt. Commun.* **1995**, *119*, 341.
(27) Kano, H.; Wada, K.; Kawata, S. *Extended Abstracts of the 43rd Spring Meeting of the Japan Society of Applied Physics and Related Societies*, 1996; p 886.
(28) Hibino, J. *Extended Abstracts of Basic Technologies for Future Industries, 1st Symposium on Photonics Materials* 1990; p 173.
(29) Ando, E.; Miyazaki, J.; Morimoto, K. *Thin Solid Films* **1985**, *133*, 21.
(30) Hamano, M.; Irie, M. *Jpn. J. Appl. Phys.* **1996**, *35*, 1764.
(31) Irie, M.; Mohri, M. *J. Org. Chem.* **1988**, *53*, 803.
(32) Denk, W.; Strickler, J. H.; Webb, W. W. *Science* **1990**, *248*, 73.
(33) Kawata, Y.; Ishitobi, H.; Kawata, S. *Opt. Lett.* **1998**, *23*, 756.
(34) Sekkat, Z.; Knoll, W. *J. Opt. Soc. Am. B* **1995**, *12*, 1855.
(35) Watanabe, O.; Tsuchimori, M.; Okada, A. *J. Mater. Chem.* **1996**, *6*, 1487.
(36) Egami, C.; Suzuki, Y.; Sugihara, O.; Okamoto, N.; Fujimura, H.; Nakagawa, K.; Fujiwara, H. *Appl. Phys. B* **1997**, *64*, 471.
(37) Wang, C.; Fei, H.; Yang, Y.; Wei, Z.; Qui, Y.; Chen, Y. *Opt. Commun.* **1999**, *159*, 58.
(38) Ishikawa, M.; Kawata, Y.; Egami, C.; Sugihara, O.; Okamoto, N.; Tsuchimori, M.; Watanabe, O. *Opt. Lett.* **1998**, *23*, 1781.
(39) Watanabe, O.; Tsuchimori, M.; Okada, A.; Ito, H. *Appl. Phys. Lett.* **1997**, *71*, 750.
(40) Tsuchimori, M.; Watanabe, O.; Ogata, S.; Okuda, A. *Jpn. J. Appl. Phys.* **1997**, *36*, 5518.
(41) Day, D.; Gu, M. *Appl. Opt.* **1998**, *37*, 6299.
(42) Cheng, P. C.; Bhawalkar, J. D.; Pan, S. J.; Swiatkiewicz, J.; Samarabandu, J. K.; Liou, W. S.; He, G. S.; Ruland, G. E.; Kumar, N. D.; Prasad, P. N. *Scanning* **1996**, *18*, 129.
(43) Dvornikov, A. S.; Rentzepis, P. M. *Opt. Commun.* **1997**, *136*, 1.
(44) Hell, S.; Booth, M.; Wilms, S.; Schnetter, C.; Kirsh, A.; Arndt-Jovin, D.; Jovin, T. *Opt. Lett.* **1998**, *23*, 1238.
(45) Gu, M.; Day, D. *Opt. Lett.* **1999**, *24*, 288.
(46) Fermann, M. E.; Hofer, M.; Haberl, F.; Schmidt, A. J. *Opt. Lett.* **1991**, *16*, 244.
(47) Fermann, M. E.; Yang, L. M.; Stock, M. L.; Andrejco, J. M. *Opt. Lett.* **1994**, *19*, 43.
(48) Yamada, E.; Yoshida, E.; Kitoh, T.; Nakazawa, M. *Electron. Lett.* **1995**, *31*, 1324.
(49) Fermann, M. E.; Galvanauskas, A.; Harter, D.; Minelly, J. D. *Optical Fiber Communications Conference*, San Jose, CA, 1998.
(50) Hansen, P. B.; Raybon, G.; Koren, U.; Miller, B. I.; Young, M. G.; Newkirk, M. A.; Chien, M. D.; Tell, B.; Burrus, C. A. *Electron. Lett.* **1993**, *29*, 739.
(51) Nirmalathas, A.; Liu, H. F.; Ahmed, Z.; Pelusi, M. D.; Novak, D. *Proc. IEEE Int. Semiconductor Laser Conf.* **1996**, p 53.
(52) Arahira, S.; Matsui, Y.; Kunii, T.; Oshiba, S.; Ogawa, Y. *IEEE Photon. Technol. Lett.* **1996**, *32*, 1211.
(53) Wilson, T.; Sheppard, C. J. R. *Theory and Practice of Scanning Optical Microscopy*; Academic Press: London, 1984.
(54) Nakamura, O.; Kawata, S. *J. Opt. Soc. Am. A* **1990**, *7*, 522.
(55) Wilson, T. *Confocal Microscopy*; Academic Press: London, 1990.
(56) Kawata, Y.; Juskaitis, R.; Tanaka, T.; Wilson, T.; Kawata, S. *Appl. Opt.* **1996**, *35*, 2466.
(57) Streibl, N. *J. Opt. Soc. Am. A* **1985**, *2*, 121.
(58) Sheppard, C. J. R. *Optik* **1986**, *74*, 128.
(59) Sheppard, C. J. R.; Gu, M.; Mao, X. Q. *Opt. Commun.* **1991**, *81*, 281.
(60) Wilson, T.; Kawata, Y.; Kawata, S. *Opt. Lett.* **1996**, *21*, 1003.
(61) Sekkat, Z.; Pretre, P.; Knoesen, A.; Volksen, W.; Lee, V. Y.; Miller, R. D.; Wood, J.; Knoll, W. *J. Opt. Soc. Am. B* **1998**, *15*, 401.
(62) Gibbson, W. M.; Shannon, P. J.; Sun, S. T.; Swetlin, B. J. *Nature* **1991**, *351*, 49.
(63) Andderle, K. *Liq. Cryst.* **1991**, *9*, 691.
(64) Todorov, T.; Nikolova, L.; Tomova, N. *Appl. Opt.* **1984**, *23*, 4309.
(65) Ebralidze, T. D.; Mumladze, A. N. *Appl. Opt.* **1990**, *29*, 446.
(66) Albota, M.; Beljonne, D.; Bredas, J. L.; Ehrlich, J. E.; Fu, J. Y.; Heikal, A. A.; Hess, S. E.; Kogej, T.; Levin, M. D.; Marder, S. R.; McCord-Maughon, D.; Perry, J. W.; Rockel, H.; Rumi, M.; Subramaniam, G.; Webb, W. W.; Wu, X. L.; Xu, C. *Science* **1998**, *281*, 1653.

CR980073P